DOI: 10.15587/978-617-7319-49-7.CH8

8 RESEARCH OF STRESS-STRAIN STATE OF ELEMENTS OF TECHNOLOGICAL TECHNICAL CONSTRUCTIONS

I. Nazarenko, O. Dedov, M. Delembovskyi,
Ye. Mishchuk, M. Nesterenko, I. Zalisko, V. Slipetskyi

ABSTRACT

The distribution of stresses and strains in the elements of vibration structures of machines has been investigated. Vibrograms of changes in the stresses of the forming surface were obtained for individual elements located near the application of a dynamic external force. Comparing the obtained results of the stress-strain state of the forming structure, a new effect of using high frequencies of the operating mode when compacting concrete mixtures was discovered. Due to the application of a spatial forced force to the forming structure, a complex stress-strain state of metal structures is created. And direct contact with the concrete mix helps to reduce energy consumption for the compaction process. The study of the motion of systems related to block structures, the adopted model, which is a two-mass vibration system. The identified transient process is intended to be taken into account when determining the parameters and locations of the vibrators. In such modes, the forms of natural vibrations of the system are realized with large vibration amplitudes and, accordingly, a lower frequency. And this opened up a real opportunity to reduce the energy consumption of vibration machine drives. The stress-strain state of the frame and forms of a vibration unit with spatial vibrations has been investigated. The distribution of stresses in the frame elements is uneven. The concentration of stresses in the welding places of elements having small values in comparison with the ultimate strength of steel has been determined. The static and dynamic loads of the slewing ring of a truck crane have been investigated. The positions of the system and its elements with the highest stresses are established. The results obtained were used in the design of the metal structures of the machines under study.

KEYWORDS

Metal structure, vibration system, stress-strain state, form-generating structure, model, numerical calculations, natural vibration modes, vibrator, spatial vibrations, truck crane, slewing ring.

8.1 STATEMENT OF TASKS AND RESEARCH METHODS

Studying the distribution of stresses and deformations in structural elements of vibration machines will allow analyzing and identifying places of stress concentration, which allows optimization of design solutions.

Based on the existing methods and a certain mathematical description (see Section 2), the problem arises of specifying the constituent elements of the pre-static and dynamic action of the load determined in the study of the machine-medium systems.

Thus, the formulation of the problem of computer modeling is reduced to the construction of a system that replaces and reflects the actual system, and in cognitive processes is in the corresponding similarity with it.

In the general case, any existing or created object can be considered in three-dimensional space both under static and dynamic action on it [1, 2]. Since the entire system is three-dimensional [3, 4], then all elements belonging to it also have three coordinates of displacements and three angles of rotation relative to the axes, that is, six degrees of freedom (DOF).

In accordance with the principles of modeling, the determination of the structural parameters of the elements is based on the ratio of the geometric dimensions and the type of arising (possibly arising) stresses in the structural elements.

So, to simulate a structural element located only in the field of tensile – compression forces (provided that it works in the zone of elastic deformations) and its length with respect to the cross section differs by an order of magnitude, it is enough to consider a one-dimensional problem. Since the processes occurring within the section can be neglected. The model that will reflect the behavior of such a system will look like a bar, the ends of which are clamped by a fixed and movable hinge, respectively.

For structural elements that are in the field of complex types of forces and the ratio of overall dimensions to plane to height are within several orders of magnitude, a system of two-dimensional elements with a thickness – plates – should be considered. Accordingly, structural elements that have overall dimensions of the same order and (or) are in a complex stress-strain state are considered volumetric elements and, accordingly, the system (model) is considered three-dimensional.

Knowledge of the stresses in the sealing layers under the action of a force load allows one to determine the sealing zone and, as a result, to determine the parameters of the sealing equipment with sufficient reasoning.

Improvement of the structures of vibration machines is possible by simulating the operation of this structure under loading, starting from the stage of an unloaded structure and ending with its full load [5, 6]. The study of displacements and deformations of structural elements of technological machines will allow identifying places of stress concentration and optimizing design solutions using finite element analysis [7].

At all nodes, generalized coordinates λ_1 are specified, called nodal offsets, the totality of which for a given element is written in the form of a matrix:

$$\{\lambda\} = \{\lambda_1, \lambda_2, \ldots, \lambda_N\}^T, \tag{8.1}$$

where N – total number of node displacements of the element; the sign T means the transposition of the matrix. Nodal displacements can represent the components of the vector of displacement of the nodes along the coordinate axes, as well as the angles of rotation of the element at the nodal points.

Within each element, for the components of the displacement vector of any point M, an approximation is set in terms of nodal displacements, which are unknown quantities:

$$u_i = \Phi_{ik}(M)\lambda_k,\ i = 1,2,3,\ k = 1,2...N; \tag{8.2}$$

the same in matrix notation $\{u\} = \{\Phi\}\{\lambda\}$ and vector form:

$$\vec{u} = \Phi_{ik}\vec{e}_k\lambda_k = \{\vec{\Phi}\}\{\lambda\}, \tag{8.3}$$

where $\Phi_{ik}(M)$ values are called functions of the shape of the element and express the relationship between the nodal displacements and the displacement of the point M of the body; polynomials are usually used as a shape function; outside the element, these functions are set equal to zero; $\vec{\Phi}_k = \Phi_{ik}\vec{e}_i$, $\{\vec{\Phi}\} = \{\vec{\Phi}_1, \vec{\Phi}_2, ..., \vec{\Phi}_N\}$, $\vec{e}_i$ – unit vectors.

Relations (8.3) are substituted into the body equilibrium equation, from which the nodal displacements $\{\lambda\}$ for each element are determined.

When using the finite element method, it is most convenient to obtain the body balance equation based on the principle of possible displacements. Let $\vec{u}$ is the field of displacements of points of a deformable body under the action of external loads applied to it. By setting each point a small displacement $\delta\vec{u}$ allowed by the constraints imposed on the body (movement is possible). According to this principle, the increase in the work of internal forces is equal to the work of external forces on possible displacements, i.e.:

$$\delta U = \delta W. \tag{8.4}$$

Denoting as $\vec{q}$ the external load distributed over the volume of the body V, and as $\vec{p}$ – the load distributed over its surface S.

Let's obtain:

$$\delta W = \int_V \vec{q}\cdot\delta\vec{u}\,dV + \int_S \vec{p}\cdot\delta\vec{u}\,dS. \tag{8.5}$$

The expression for the work of internal forces has the form:

$$\delta U = \int_V \sigma\cdot\delta\varepsilon\,dV, \tag{8.6}$$

where $\sigma = \sigma_{ij}\vec{e}_i\vec{e}_j$ – stress tensor; $\varepsilon = \varepsilon_{ij}\vec{e}_i\vec{e}_j$ – strain tensor; $\vec{e}_i$ – unit unit vectors, i, j=1, 2, 3.

Then relation (8.4) takes the form:

$$\int_V \sigma\cdot\delta\varepsilon\,dV = \int_V \vec{q}\cdot\delta\vec{u}\,dV + \int_S \vec{p}\cdot\delta\vec{u}\,dS. \tag{8.7}$$

In the case of small deformations of the body:

$$\varepsilon = \nabla\vec{u}, \tag{8.8}$$

where

$$\nabla\vec{u} = \frac{1}{2}\left(\frac{\partial u_i}{\partial x_j} + \frac{\partial u_j}{\partial x_i}\right)\vec{e}_i\vec{e}_j$$

– tensor operator; $i, j=1, 2, 3$; x_1, x_2, x_3 – coordinate axes directed along the unit vectors $\vec{e}_1, \vec{e}_2, \vec{e}_3$.

Substituting (8.2) into (8.8), let's obtain an expression for the components of the strain tensor in terms of the nodal displacements:

$$\varepsilon_{ij} = \frac{1}{2}\left(\frac{\partial\Phi_{ik}}{\partial x_j} + \frac{\partial\Phi_{jk}}{\partial x_i}\right)\lambda_k. \tag{8.9}$$

or in matrix form:

$$\{\varepsilon\} = \{B\}\{\lambda\}, \tag{8.10}$$

where

$$\{B\} = \{\nabla\bar{\Phi}\} = \left\{\frac{1}{2}\left(\frac{\partial\Phi_{ik}}{\partial x_j} + \frac{\partial\Phi_{jk}}{\partial x_i}\right)\right\}$$

– matrix associates deformations with nodal displacements. The relationship between the components of stress and strain tensors for an elastic body is expressed by a law:

$$\sigma_{ij} = D_{ijkl}\varepsilon_{kl}, \tag{8.11}$$

where D_{ijkl} – the elastic constants of the body, $i, j, k, l=1, 2, 3$, or in matrix form $\{\sigma\} = \{D\}\{\varepsilon\}$.

Substituting expression (8.30), let's find the dependence of the stress tensor on nodal displacements:

$$\{\sigma\} = \{D\}\{B\}\{\lambda\}. \tag{8.12}$$

After transformations, let's obtain the equation of equilibrium of an elastic body containing the movement of its points:

$$\int_V D\nabla\vec{u}\cdot\delta(\nabla\vec{u})\mathrm{d}V = \int_V \vec{q}\cdot\delta\vec{u}\mathrm{d}V + \int_S \vec{p}\cdot\delta\vec{u}\mathrm{d}S. \tag{8.13}$$

Let's apply relation (8.13) to a finite element with some volume V_e bounded by the surface S_e, and find:

$$\delta\lambda_i \left\{ \int_{V_e} \nabla\vec{\Phi}_i \cdot D\nabla\vec{\Phi}_j \cdot \lambda_j dV - \int_{V_e} \vec{q}\vec{\Phi}_i dV - \int_{S_e} \vec{p}\vec{\Phi}_i dS \right\} = 0, \tag{8.14}$$

where $i, j = 1,2,\ldots,N$.

Since $\delta\lambda_i$ – arbitrary nonzero values, the last equality requires all expressions in curly braces to rotate to zero. From these conditions, let's obtain a system of linear algebraic equations expressing the equilibrium conditions for a finite element:

$$\{K\}\{\lambda\} = \{f\}, \tag{8.15}$$

where $K_{ij} = \int \nabla\vec{\Phi}_V \cdot D\nabla\vec{\Phi}_j dV$ – stiffness matrix of the element, which, using relations (8.10) and (8.12), can also be written in the form: $\{K\} = \{B\}^T \{D\}\{B\}$;

$$f_i = \int_{V_e} \vec{q} \cdot \vec{\Phi}_i dV + \int_{S_e} \vec{p} \cdot \vec{\Phi}_i dS$$

– vector of nodal forces of the element, where $i, j = 1,2,\ldots,N$.

The set of equations (8.15) for all elements is supplemented by the equations of ligatures imposed on the body (limiting conditions), which are a system of equations for the equilibrium of the body under consideration, written in a form similar to (8.35):

$$\{\bar{K}\}\{\bar{\lambda}\} = \{\bar{f}\}, \tag{8.16}$$

where $\{\bar{K}\}$ is called the global body stiffness matrix; $\{\bar{\lambda}\}$ and $\{\bar{f}\}$ – vectors of nodal displacements and forces of the whole body.

Equations of the type (8.16) are used for strength analysis of structures under static load. From their solution, the vector of nodal displacements is determined, then, according to relation (8.2), one can find the displacement of the points of the body, and according to (8.8)–(8.11) or (8.13) – deformations and stresses.

From (8.15) it is easy to obtain the equation of motion of the element. By introducing, according to the d'Alembert principle, the volumetric forces of inertia into the integral for the nodal forces (8.15):

$$\vec{q}^{in} = -\rho \frac{\partial^2 \vec{u}}{\partial t^2} = -\rho\vec{\Phi}_j \cdot \vec{\lambda}_j, \tag{8.17}$$

let's obtain a system of equations:

$$\{M\}\{\ddot{\lambda}\}+\{K\}\{\lambda\}=\{f\}, \tag{8.18}$$

where $M_y=\int \rho\vec{\Phi}_i\cdot\vec{\Phi}_j dV$ – mass matrix of the element; ρ – material density; $\ddot{\lambda}$ – the second time derivative of the vector of nodal displacements. In the presence of viscous resistance forces in the system, proportional to the speeds of the points, the matrix of damping coefficients $\{B\}$ is introduced into (8.38), after which the equations of motion take the form:

$$\{M\}\{\ddot{\lambda}\}+\{B\}\{\dot{\lambda}\}+\{K\}\{\lambda\}=\{f\}. \tag{8.19}$$

When studying the problems of elastic resistance of structural elements, the equilibrium equation is added taking into account the change in the geometry of the body in the deformed state:

$$\left[\{\bar{K}\}-\beta\{\bar{K}_d\}\right]\{\bar{\lambda}\}=0, \tag{8.20}$$

where by means of a matrix of geometric stiffness $\{\bar{K}_d\}$, called differential in MSC.vN5W, the work of external forces due to a change in the geometry of the body is taken into account; β – loading parameter.

Equating to zero the determinant of the system (8.40) $\det\left[\{\bar{K}\}-\beta\{\bar{K}_d\}\right]=0$, let's find the value of the load parameter $\beta_1,\beta_2,\ldots$, at which there are nontrivial displacements for nodal displacements $\{\lambda\}$, i.e. new forms of body balance appear, different from the original. Such values β, called critical, show how many times the critical load F^{cr}, at which the loss of resistance of the original form of body balance occurs, is greater than the current load F:

$$F_i^{cr}=\beta_i F,\ i=1,2,\ldots \tag{8.21}$$

The first lowest critical load F_1^{cr} is usually of practical interest, since only it will be realized during the operation of the structure. To study the working process of energy-saving machines and their structural elements for the implementation of specific technological work processes, the following research sequence was established:

– justification and development of calculation schemes for the machine;
– analysis of the basic forms, amplitudes and frequencies of vibration of the structure;
– determination of modes, rational parameters to create a new highly efficient design.

8.2 INVESTIGATION AND DETERMINATION OF STRESSES AND STRAINS IN THE FORMING SURFACE OF THE STRUCTURE OF VIBRATION MACHINES

The search for constructive solutions for the creation of machines with a variable amplitude-frequency oscillation mode is to search for an increase in the efficiency of the working process.

Revealing new phenomena in the operation of compacting machines and taking them into account when modeling work processes. Improvement of models that adequately meet the real conditions of motion of a vibration machine. An effective approach in this direction is the use of continuous models, which make it possible to take into account the propagation of waves, both in the design of a vibration machine and in the compacting mixture. This approach is the basis for determining the real distribution of amplitudes and frequencies of oscillations and the use of multi-mode effects.

So, it is assumed that the design, subject to research and further creation, allows to transfer the maximum amount of energy from the working body to the medium due to the frequency spectrum with different energy components and the use of internal resonance phenomena of the system by choosing an operating mode that is coordinated in elastic-inertial and elastic-viscous properties of the machine and medium.

Thus, on the basis of the created finite element model, studies of the structure were carried out in terms of natural frequencies and vibration modes. The calculation of frequencies and modes of vibration was carried out in two stages. At the first stage, according to the nonlinear theory, static prestressing of the structure by all acting forces is performed, then at the second stage, the frequencies and, accordingly, the vibration modes are calculated.

Studying the distribution of stresses and deformations in structural elements of vibration machines will allow analyzing and identifying places of stress concentration, which allows optimization of design solutions.

To study and determine the stresses and strains in accordance with the goal, the task of calculating the supporting structures of the system in its more critical states is posed. Therefore, for research, the design of a vibration unit was selected, which is a form-forming surface for compacting a concrete mixture. The structure consists of a welded box-section frame mounted on rubber resilient supports and a metal sheet as a shaping surface. Loads of auxiliary structural elements and concrete mix were included in the dynamic component of forces.

The total number of finite elements turned out to be 59 856, the number of nodes – 100 998. It is assumed that the structure frame is rigidly fixed on rubber supports and the materials of all elements are deformed only in the elastic stage.

The nature of the stress-strain state of the structure under the action of external forces and gravity is illustrated in color in **Fig. 8.1**.

The scale of displacement values corresponding to this palette is represented on the left in the form of a colored column. As follows from **Fig. 8.1** the maximum values of the equivalent stresses of the forming surface are 2.5 MPa. Higher values of stresses are concentrated in the area of application and distribution of the driving force.

The frame design accepts a maximum stress of 11.7 MPa (**Fig. 8.2**). The area of action of such stress values is limited by the contact zones of the frame with the supports and is of a local nature. In general, the frame of the structure is in a state of uniform stress distribution.

In order to study the behavior of the forming surface under dynamic action, the distribution of stresses in time is analyzed. In particular, **Fig. 8.3** shows vibrograms of changes in the stresses

of the forming structure for individual elements located near the application of a dynamic external force. As seen from **Fig. 8.3**, at the beginning, a transient process was detected, caused by the exit of the system from a state of rest into oscillatory motion. An increase in the amplitude of stress changes at this stage is a consequence of the transition of the system through resonance modes at lower vibration frequencies.

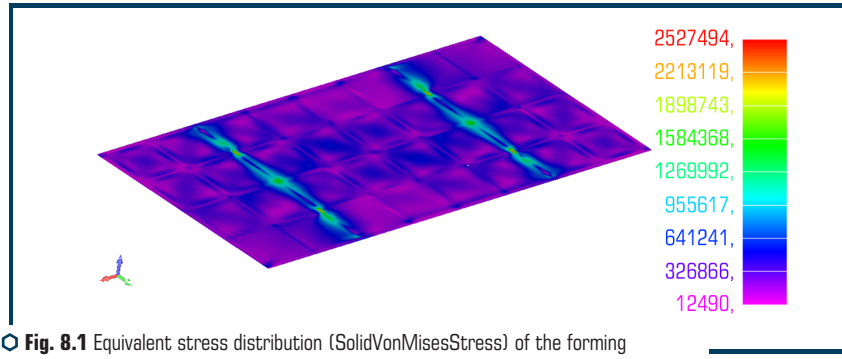

Fig. 8.1 Equivalent stress distribution (SolidVonMisesStress) of the forming surface (time 0.0748 s)

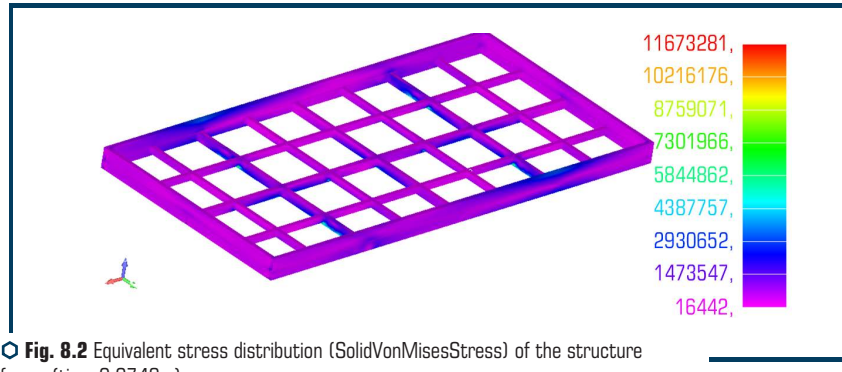

Fig. 8.2 Equivalent stress distribution (SolidVonMisesStress) of the structure frame (time 0.0748 s)

In such modes, the forms of natural vibrations of the system are realized with large vibration amplitudes and, accordingly, a lower frequency. When the operating mode is set, negative stress arise in structural element 18 857. The nature of the change in these stresses is periodic and antiphase in comparison with the applied spatial force. The stress of element 48 345 are positive and vary with an offset of $\pi/2$ relative to the applied force. This dependence is explained by the spatial arrangement of the elements in relation to the point of application of the force. But the nature of the change in this force of the force load, since it changes along the two axes of space.

For structural elements 48 114 and 17 290, which are located symmetrically on the opposite side of the applied force, the nature of the change is shown in **Fig. 8.4**. In contrast to the previous vibrograms, one can see the absence of in-phase changes in stress in relation to the forced force. The significant difference can be explained by the dissipation phenomena occurring in the structure.

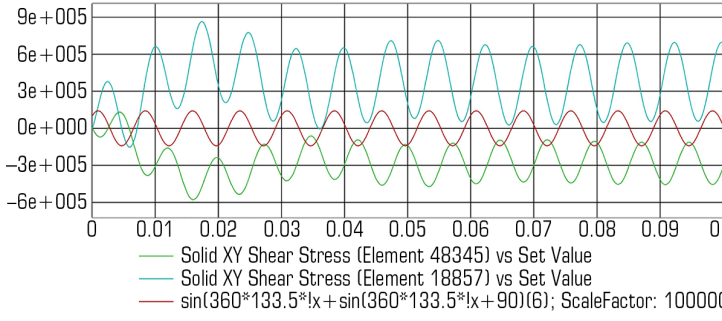

Fig. 8.3 Dependence of shear stresses (Solid XY ShearStress) of the forming surface (elements 48 345 and 18 857) and the vertical component of the driving force

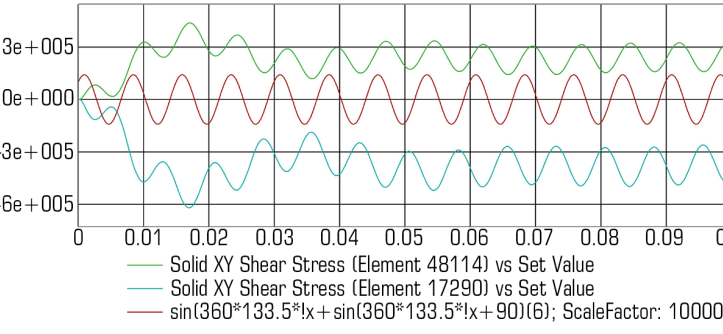

Fig. 8.4 Dependence of shear stresses (Solid XY ShearStress) of the forming surface (elements 48 114 and 17 290) and the vertical component of the driving force

It is quite obvious that the change in the stress-strain state of the system under study is rather difficult. Such a change is associated with the implementation of complex spatial vibrations and the multi-mode of the sealing process. An important criterion for evaluating a design from the point of view of the efficiency of the compaction process is shear stress. Indeed, in the presence of such stresses in the medium, there is an intensive movement of particles and compaction.

To analyze the shear stresses of the forming surface, time intervals are selected that correspond to 1/4 of the period of oscillation of the driving force. **Fig. 8.5** shows the distribution of stresses in the *XY* plane at a time of 0.0748 s, which is taken as a relative origin.

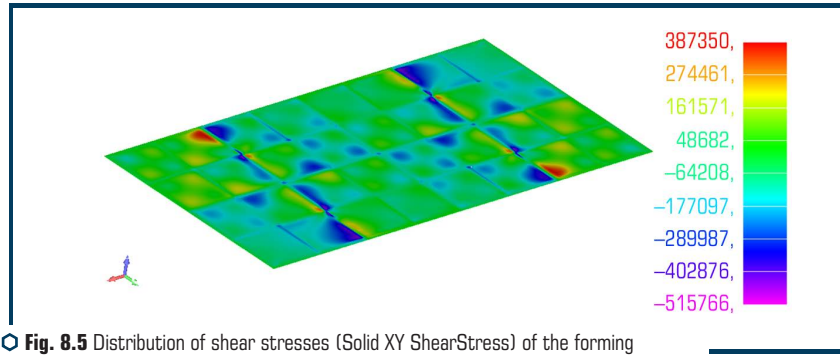

Fig. 8.5 Distribution of shear stresses (Solid XY ShearStress) of the forming surface (time 0.0750 s)

This is evidenced by the zones with the maximum positive stress values, in which the force is applied. The entire surface is in a complex sign-like stress-strain state.

When the force is turned by an angle of $\pi/4$, the stress distribution changes (**Fig. 8.6**). The appearance of additional zones of maximum stresses indicates the transfer of the load in the horizontal direction and the presence of bending and torsional vibrations. In this case, the middle of the structure is at relative rest.

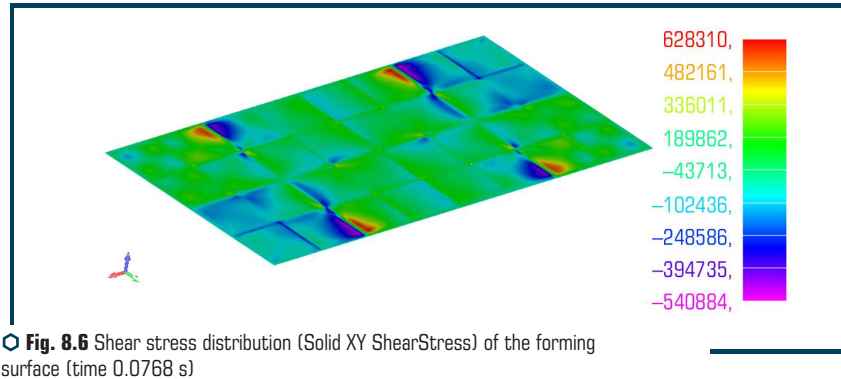

Fig. 8.6 Shear stress distribution (Solid XY ShearStress) of the forming surface (time 0.0768 s)

When the force returns to an angle of $\pi/4$, almost the entire surface of the forming surface is disturbed (**Fig. 8.7**). Deformation and stress have a sign-like character indicating the presence

of wave phenomena. The transfer of stresses occurs in the direction of the diagonal connecting the points of application of external dynamic forces.

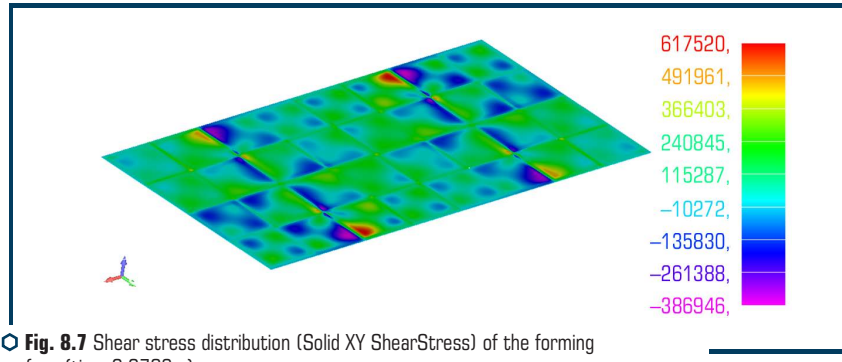

Fig. 8.7 Shear stress distribution (Solid XY ShearStress) of the forming surface (time 0.0786 s)

In the period of time 0.0806 s (3/4π), the propagation of oscillations continues, as evidenced by a change in the stress distribution (**Fig. 8.8**). Deformation and stress are alternating in nature, as in the previous period of time, but their stress distribution is more uniform and orderly. It should be noted that there are zones in the corners of the forming surface. In these zones, the change in stresses is less intense and most of the surface perceives positive stress values. At the same time, the number of surface areas with negative stress values is insignificant.

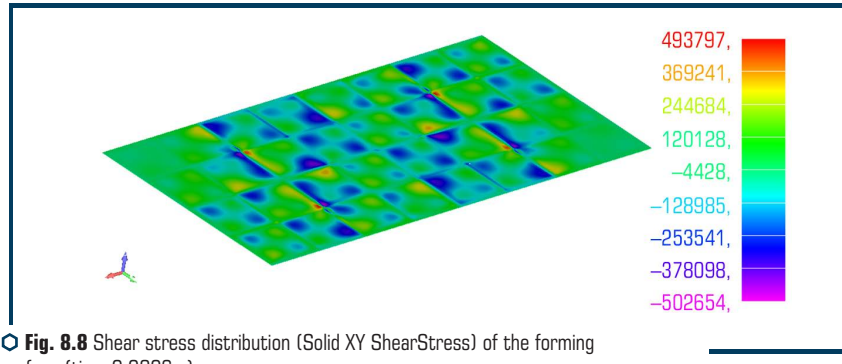

Fig. 8.8 Shear stress distribution (Solid XY ShearStress) of the forming surface (time 0.0806 s)

Comparing the obtained results of the stress-strain state of the forming structure, the following can be noted. The use of high frequencies of the operating mode will allow obtaining a new effect when compacting concrete mixtures. Due to the application of a spatial forced force to the forming

structure, a complex stress-strain state of metal structures is created. And direct contact with the concrete mix helps to reduce energy consumption for the compaction process.

To study the motion of systems related to block structures, a model was adopted (**Fig. 8.9**), which is a two-mass vibration system. The lower mass of the system consists of four vibration blocks resting on elastic elements calculated according to the vibration isolation conditions.

The upper mass simulates the shape with the medium to be processed. Between the upper and lower masses there are elastic elements, the stiffness of which is taken from the condition for the realization of the resonant mode of motion and providing the technological process.

In order to carry out research, the following overall dimensions of the structure were adopted:

– total length 3.30 m;

– width 0.50 m;

– height 0.34 m.

The model was investigated by the finite element method. The finite element model of the structure was compiled by approximating all load-bearing elements, including the forming surface, with two-dimensional finite elements of the PLATE type, elastically deformed under the action of a longitudinal force, bending moments in two planes and a torque.

Vibration isolation supports and elastic elements of the model are adopted as three-dimensional CE of the SOLID type, since the processes occurring in such structural elements are more complex in terms of energy dissipation.

The total number of finite elements was 19 258, the number of nodes was 19 912, and the total number of searched variables was 20 928.

It is assumed that at the extreme points, the supports rest on the foundation and are fixed, therefore, in the model, the extreme nodes of the supports are restrained in the *X*, *Y*, *Z* directions, and rotations in all three axes are also prohibited.

It is believed that the materials of the entire structure are deformed only in the elastic stage.

When checking the strength and determining the functioning of a system that can be subjected to loads that are different in their nature and applied in various combinations, it is advisable to first analyze the behavior of the structure under the simplest loads, and then complicate them with the addition of other disturbances.

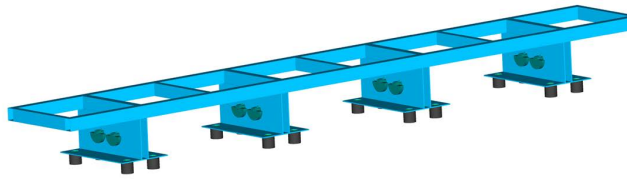

Fig. 8.9 Model of block vibration unit

To check the model and assess its functioning under the action of static and dynamic loads, the following research stages were taken:

– static calculation under the action of the weight of structural elements and the equivalent load of the medium being processed;

– modal analysis;

– dynamic analysis of the structure under the action of a forced force with a vibration frequency close to the natural vibration frequency.

The studies of the unit (**Fig. 8.10**) were carried out in several stages. at the first stage, a modal analysis was carried out in order to determine the main forms and the corresponding vibration frequencies.

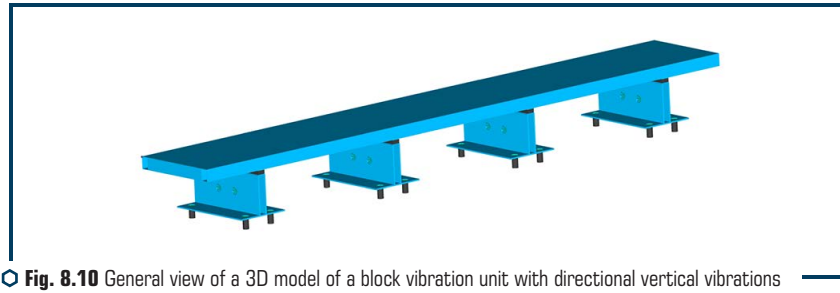

Fig. 8.10 General view of a 3D model of a block vibration unit with directional vertical vibrations

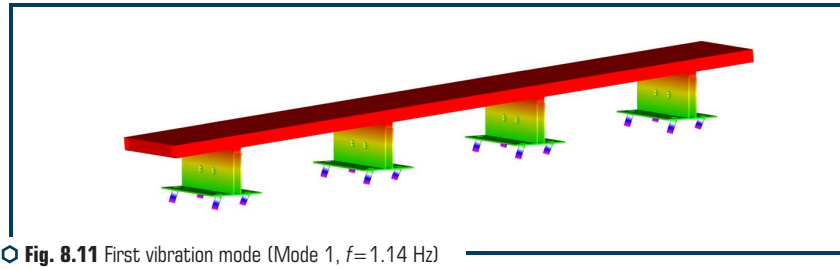

Fig. 8.11 First vibration mode (Mode 1, f=1.14 Hz)

So, at an oscillation frequency f=1.14 Hz (**Fig. 4.12**), f=1.32 Hz (**Fig. 8.12**), the vibration unit will vibrate in the first and second modes of vibration in the horizontal plane (*XY*). This mode of vibration is due to the value of the stiffness of elastic supports, which in the horizontal direction have an insignificant stiffness due to geometric features and physical and mechanical characteristics.

Fig. 8.13 shows the operating mode of the unit at an oscillation frequency f=2.57 Hz. In this mode, vibrations are performed in the horizontal plane and have a twisting character.

When the mode is realized at a frequency of f=4.10 Hz (**Fig. 8.14**), the oscillations are directional in the vertical direction. This mode corresponds to the resonant mode of vibration, when the vibration frequency corresponds to its own frequency on vibration isolation elastic elements.

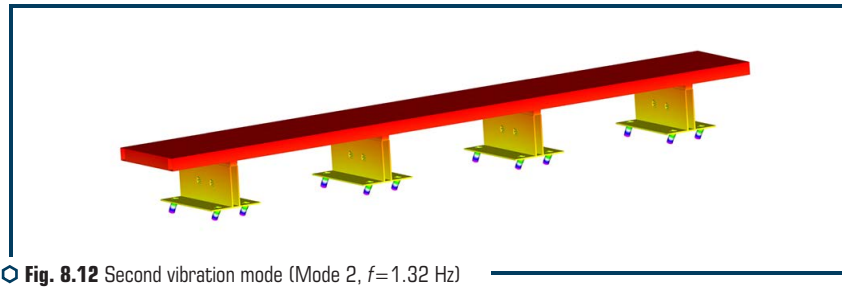

Fig. 8.12 Second vibration mode (Mode 2, $f=1.32$ Hz)

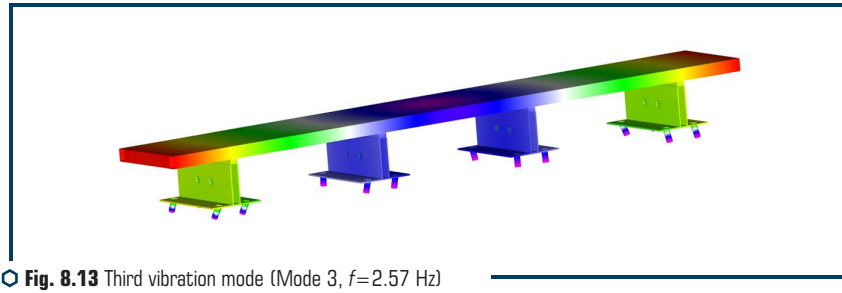

Fig. 8.13 Third vibration mode (Mode 3, $f=2.57$ Hz)

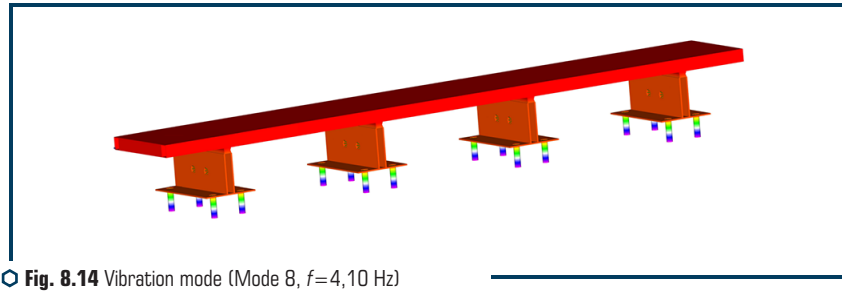

Fig. 8.14 Vibration mode (Mode 8, $f=4,10$ Hz)

The implementation of oscillations according to the mode at a frequency of $f=16.61$ Hz (Mode 23) is a consequence of the influence of the rigidity of the form (**Fig. 8.15**). Oscillations occur due to the bending of the structure in the *YZ* plane. Such modes are insufficient for the process of compaction of concrete mix. Purely unidirectional oscillations with low frequencies do not cause stresses in the medium that do not exceed the voltage loss of continuity. The operating mode, in which the phase displacement will be realized, is possible when increasing to a frequency of $f=27.40$ Hz (**Fig. 8.16**). This is due to the fact that with increasing frequency, the numerical values of the compressive stresses of the mixture layers and the rupture stress of the layers increase significantly. Also, this mode implements vibrations of the shaping surface, which are realized on elastic elements.

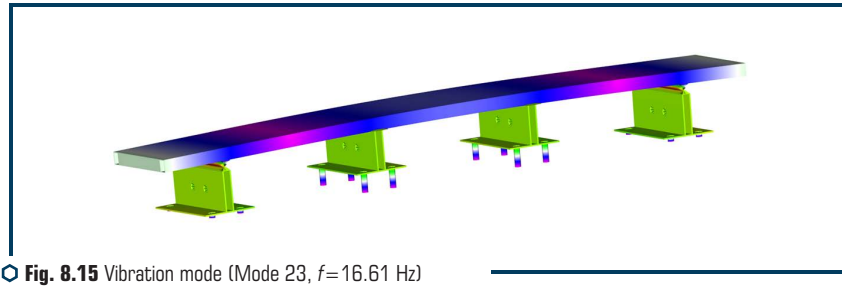

Fig. 8.15 Vibration mode (Mode 23, f=16.61 Hz)

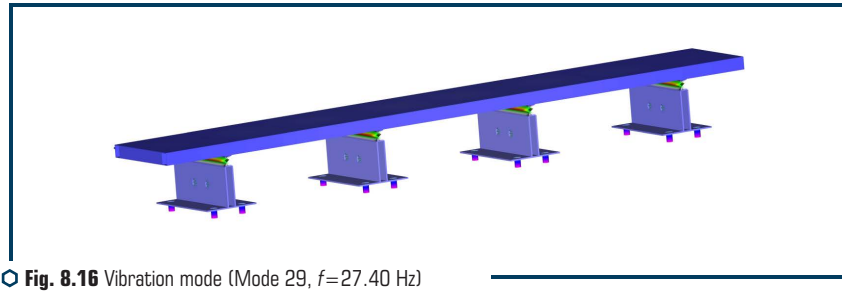

Fig. 8.16 Vibration mode (Mode 29, f=27.40 Hz)

A further increase in vibration frequencies and the implementation of the corresponding vibration modes leads to vibrations of the vibration unit form (**Fig. 8.17**), which is explained by the sufficient stiffness of the form frame and the corresponding stiffness of elastic elements (rubber gaskets).

Since the operating mode of such structures is considered as close to resonance, the choice of the operating mode must be carried out in such a way that the value of the operating frequency is 0.90–0.95 of the natural frequency.

Thus, the operating mode is adopted with a vibration excitation frequency of 25 Hz.

The implementation of the dynamic analysis was carried out in order to obtain the distribution of the vibration amplitudes of the shaping surface along the length of the structure with the application of a driving force on each vibration block.

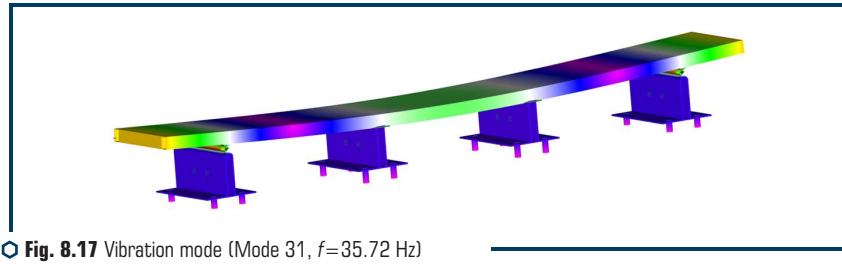

Fig. 8.17 Vibration mode (Mode 31, f=35.72 Hz)

To analyze the dynamics with directional vibrations, the values of displacements in time were obtained.

To study the behavior of the shaping surface, a list and place of points on the surface of the form were determined with the determination of the distribution of vibration amplitudes depending on the location of blocks with vibration exciters (**Fig. 8.18**).

Thus, the implementation of oscillations in one period is shown in **Fig. 8.19**.

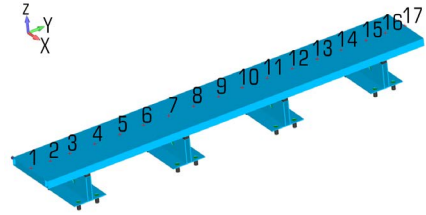

Fig. 8.18 Arrangement of control points on the surface

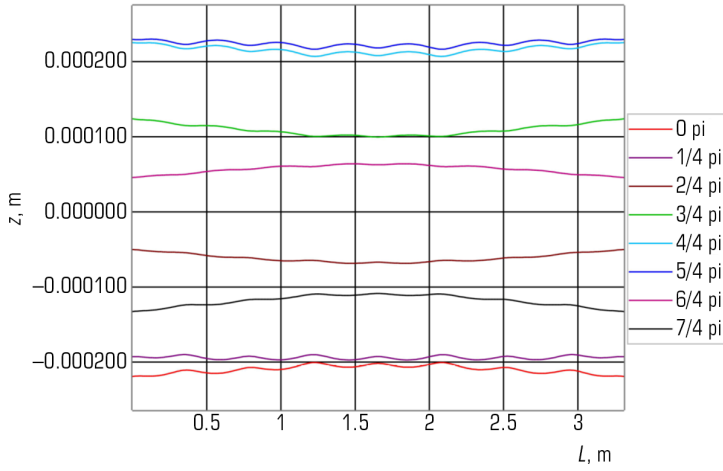

Fig. 8.19 Distribution of vertical vibrations along the length of the forming surface

As can be seen from the distribution, the oscillations are carried out in the vertical plane, which fully confirms the classical approach to modeling such systems with discrete parameters when considering a one-dimensional problem. The maximum value of the vibration amplitude is 0.22–0.25 mm.

So, the implementation of oscillations for one period is shown in **Fig. 8.20**. As can be seen from the distribution, oscillations occur in the vertical plane, which fully satisfies the classical approach to modeling such systems with discrete parameters when considering a one-dimensional problem and thus confirms the adequacy of the created model within the framework of the research. The maximum value of the vibration amplitude is 0.22–0.25 mm.

The analysis of vibrations in the horizontal direction was carried out relative to the *Y*-axis (**Fig. 8.20**), showed the practical absence of vibrations and displacements of the forming surface. The vibration amplitudes are $2 \cdot 10^{-7}$ m, which is three orders of magnitude less than in the vertical direction and it is quite obvious that such values can be neglected.

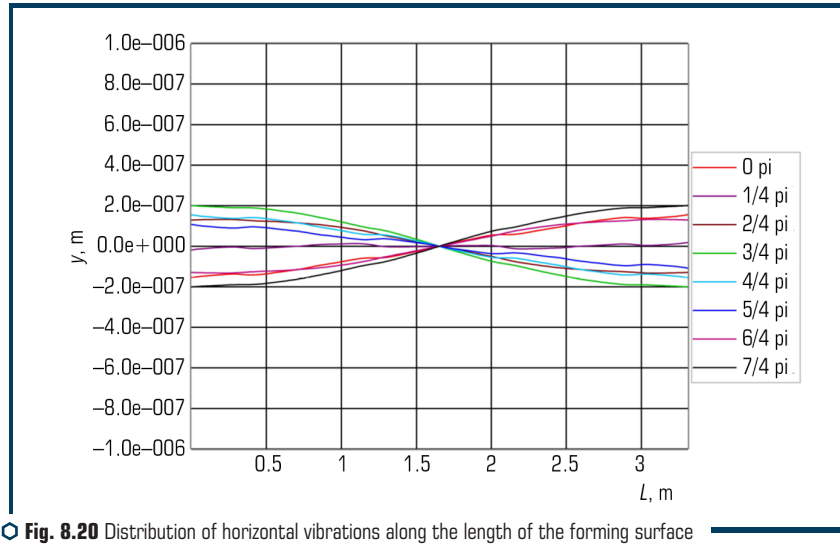

Fig. 8.20 Distribution of horizontal vibrations along the length of the forming surface

Likewise, the absence of oscillations along the *X* axis, since the forcing force is directional and does not act in this direction.

The considered mode of operation of the block structure of the vibration platform with directional vertical vibrations made it possible to analyze the distribution of amplitudes along the length of the forming surface and confirm the adequacy of the adopted model.

To implement the idea of a polyphase oscillation mode, studies of a finite element model have been carried out. Modeling of the vibration unit movement was carried out under two conditions of application of external forces: the first option provided for the application of a driving force with a shift angle of 90° on each vibration unit (**Fig. 3.2**, $\varphi_1 = 0$; $\varphi_2 = 90°$; $\varphi_3 = 180°$; $\varphi_4 = 270°$); the second variant of the load with angles $\varphi_1 = 0$; $\varphi_2 = 60°$; $\varphi_3 = 120°$; $\varphi_4 = 180°$, respectively. The frequency and value of the driving force were similar to the case of directional vertical vibrations.

So, as a result of dynamic analysis, distributions of vibration amplitudes along the *Z* (**Fig. 8.21, *a***) and *Y* (**Fig. 8.21, *b***) axes were obtained for the angle $\varphi = 90°$.

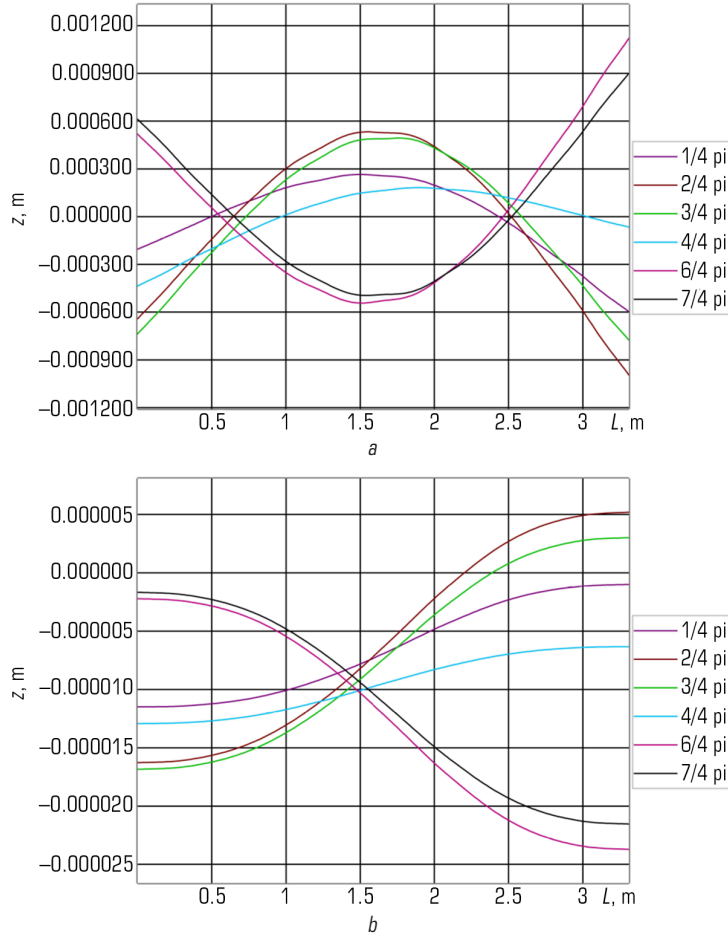

Fig. 8.21 Distribution of vibration amplitudes along the length of the structure for one period of vibration (angle=90°): *a* – *X* axis; *b* – *Y* axis

The maximum value of the vibration amplitude within the framework of the studies performed was obtained at the boundary of the form and, respectively, are 0.6 and 1.1 mm in time intervals from 3/4π to 7/4π for oscillations of the *Z* axis, and for oscillations in the Y direction – $22 \cdot 10^{-6}$ and $5 \cdot 10^{-6}$ mm.

It should be noted that there are points at which vertical vibrations occur to a much lesser extent, but at the same points there are vibrations with a horizontal component, therefore, at these points vibrations are present in both directions and there are all the conditions for compaction of the building mixture.

Distribution of vibration amplitudes at angle $\varphi = 60°$ is shown in **Fig. 8.22** in practice, it is possible to see a similar picture with the previous study, although there is a certain difference, which consists in the fact that there are no points with less vibration intensity.

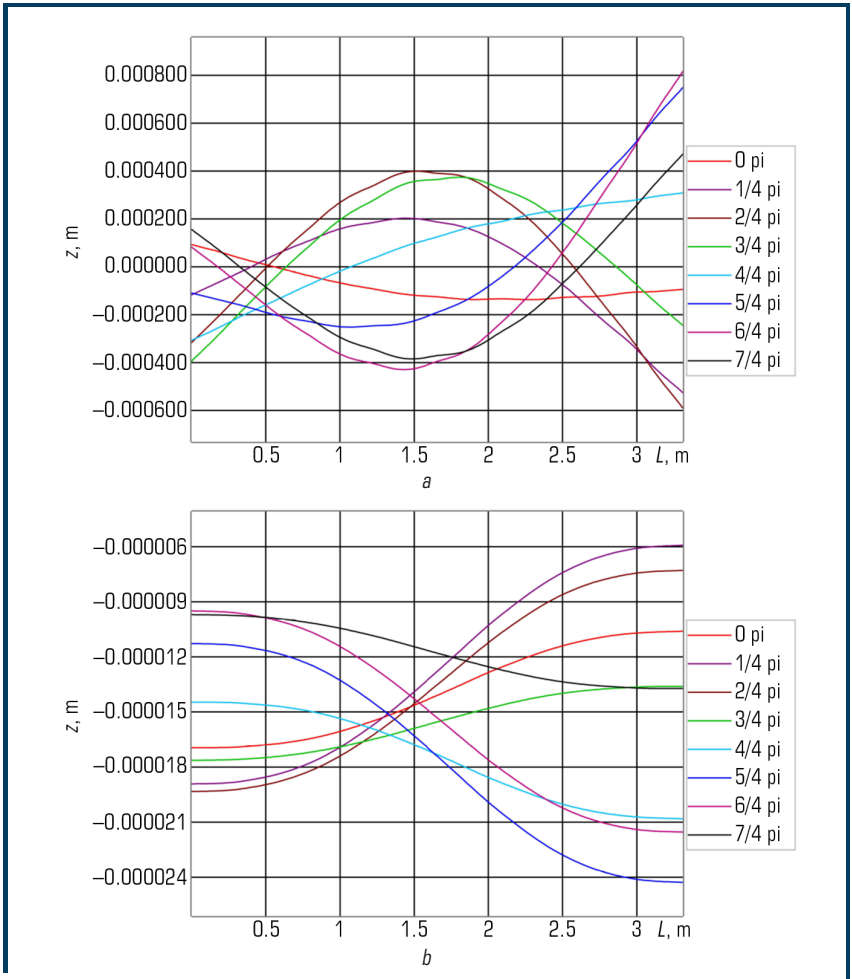

Fig. 8.22 Distribution of vibration amplitudes along the length of the structure for one period of vibration (angle = 60°): *a* – *X* axis; *b* – *Y* axis

So there are places where the displacements pass through the zero mark, but compared to the previous mode of operation, these points do not have a clear position along the length of the form, but shift with each $\pi/4$ time interval. Thus, transferring vibrations to a larger volume of concrete mix near the contact zone. It should be noted a certain increase in the amplitude of oscillations in the horizontal direction in comparison with the shear angle $\varphi = 90°$, as for vertical oscillations, that is, a decrease in the values to 0.6 and 0.8 mm.

Comparing the three operating modes of the block platform ($\varphi = 0°$, $\varphi = 60°$, $\varphi = 90°$), it is possible to note a positive contribution to the qualitative characteristic of oscillations when changing phase angles other than 0. And when comparing the general distribution of amplitudes at an angle of $\varphi = 90°$ and $\varphi = 60°$, it is obvious that it is the shift angle $\varphi = 60°$ that has the advantage.

For a more detailed study of the motion of the shaping surface with this implementation of the model (**Fig. 8.10**), let's consider modeling the motion in time.

The movement of the surface at points 1, 2, 16, 17 (**Fig. 8.18**) in time indicates the presence of different values of the vibration amplitudes (**Fig. 8.23**). So, at point 16, the amplitude of oscillations reaches 0.6 mm, and at point 2, at the same time, it has a value of 0.2 mm, which is evidence of the presence of a wave process.

At other points (**Fig. 8.24**) vibrograms of movement are identical in character to those discussed above. In terms of magnitude, the amplitudes of the oscillations are of lesser importance. At point 14, the magnitude of the amplitude reaches 0.4 mm, and at point 3, in the same period of time, the amplitude of the oscillations is 0.1 mm. At points 14 and 15, there is practically no phase displacement between the vibration amplitudes.

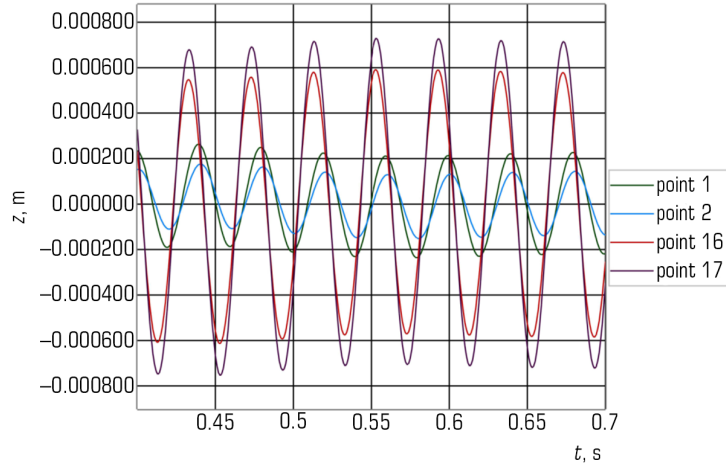

Fig. 8.23 Vibrograms of movement of points 1, 2, 16, 17 in time

Vibrograms of movement at points 5, 6, 12, 13 in time (**Fig. 4.25**) are similar in nature, as for other points (**Fig. 8.24, 8.25**).

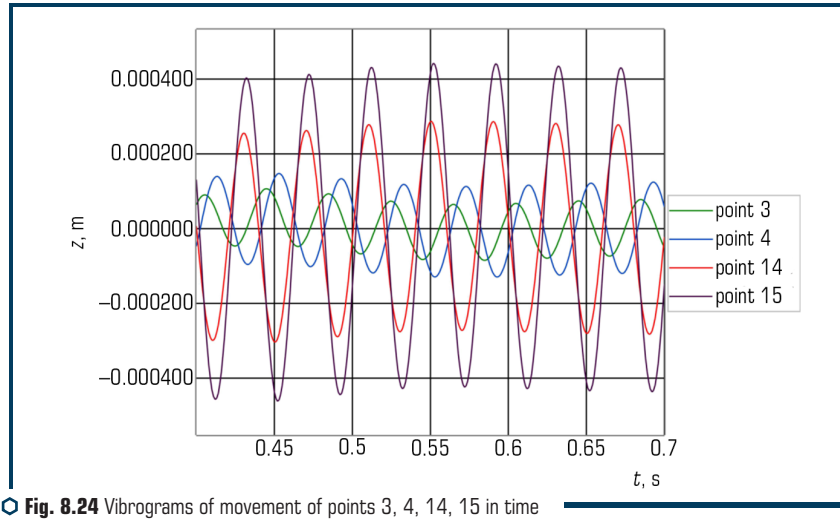

Fig. 8.24 Vibrograms of movement of points 3, 4, 14, 15 in time

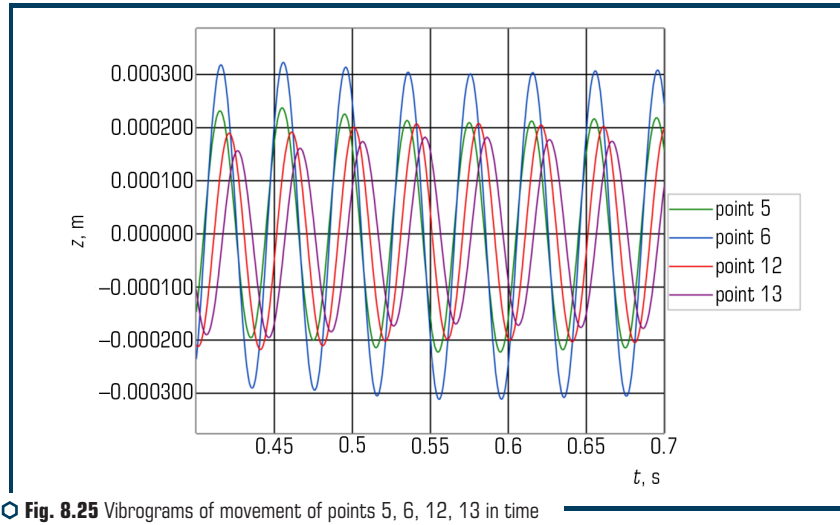

Fig. 8.25 Vibrograms of movement of points 5, 6, 12, 13 in time

However, there are also certain differences. So, it was recorded that at points 6, 12 and 13 the vibration amplitudes have similar numerical values within 0.18–0.23 mm. The change in the

oscillation amplitudes at points 7, 8, 9, 10, 11 in time (**Fig. 8.26**) is characterized by a certain deviation in numerical values and in phase.

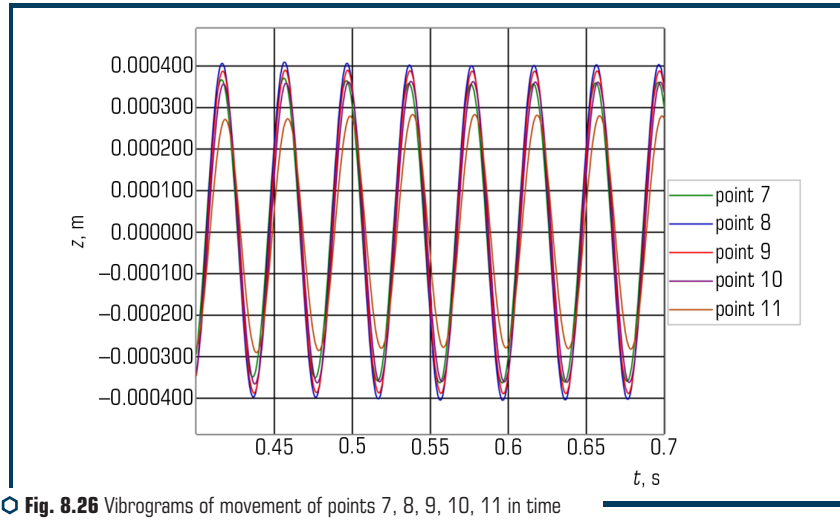

Fig. 8.26 Vibrograms of movement of points 7, 8, 9, 10, 11 in time

At these points, the amplitudes of oscillations reach values of 0.27–0.40 mm, that is, the limit of change is the smallest in comparison with the movement of points 1, 2 and 16, 17 (**Fig. 8.26**).

The research results indicate the presence of vibration amplitudes different in shape and numerical values over the area of a vibration unit with a polyphase vibration spectrum.

8.3 INVESTIGATION OF THE STRESS-STRAIN STATE OF THE FRAME AND FORMS OF A VIBRATION UNIT WITH SPATIAL VIBRATIONS

8.3.1 MODELING THE STRESS-STRAIN STATE OF VIBRATION PLATFORMS

Determination of the stress-strain state of the vibration platform frame is not an easy task. The complexity of the research is associated with various factors: an increase in the number of finite elements, the use of various types of finite elements in one numerical model, problems of mechanical properties of rubber platform supports, modeling of various types of loads (static and dynamic), modeling of welded joints of a space frame [8, 9].

The following types of finite elements can be used to calculate frames and shapes:

a) the frame elements are modeled with SOLID55 elements. The element is a three-dimensional hexagon with eight nodes located at the corners. This type of element allows the use of

isotropic, plastic and other nonlinear types of materials, with the exception of hyperelastic ones. Elements of this type can take degenerate shapes. Degenerate elements have at first a quadrangular or hexagonal shape, but by combining two or more nodes that take the shape of a triangle for flat elements or a tetrahedron, prism or wedge for volumetric ones;

b) welded seams are taken as idealized and modeled from volumetric finite elements in the form of a six-node triangular prism with the same bases equal to the leg;

c) to model rubber supports, a finite element SOLID185 is used – an element similar to SOLID55, but allows the use of hyperelastic materials.

The displacements of the lower planes of the supports are limited in the *X*, *Y*, *Z* directions, which simulates a rigid clamping of the structure in the foundation. The vibration exciters on the frame are shown conditionally, and their effect on the frame is determined by the driving force. The load on the frame from the form and the concrete mix is simulated by applying a uniformly distributed load.

8.3.2 VIBRATION PLATFORM WITH VERTICAL VIBRATOR

A vibration platform with a horizontal vibrator is divided into finite elements (**Fig. 8.27**). For it, a displacement distribution diagram was obtained (**Fig. 8.28**) in the *X*, *Y*, *Z* directions and a stress distribution diagram (**Fig. 8.29**).

The largest total displacements of the frame elements (**Fig. 8.28**) are observed in the outer frame elements, their maximum value is 0.0615 mm.

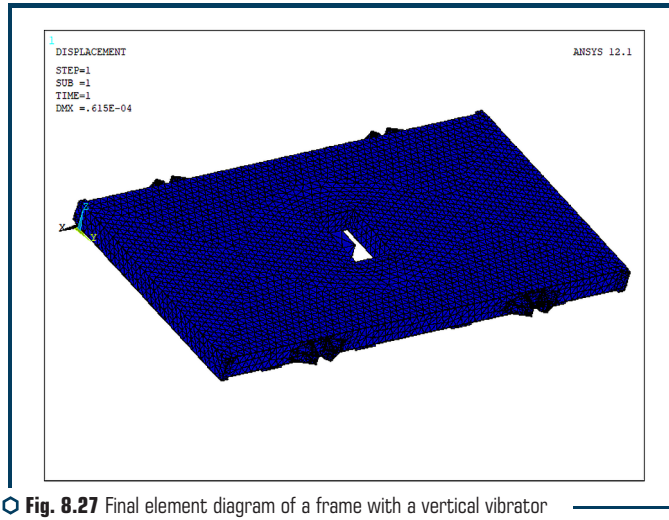

Fig. 8.27 Final element diagram of a frame with a vertical vibrator

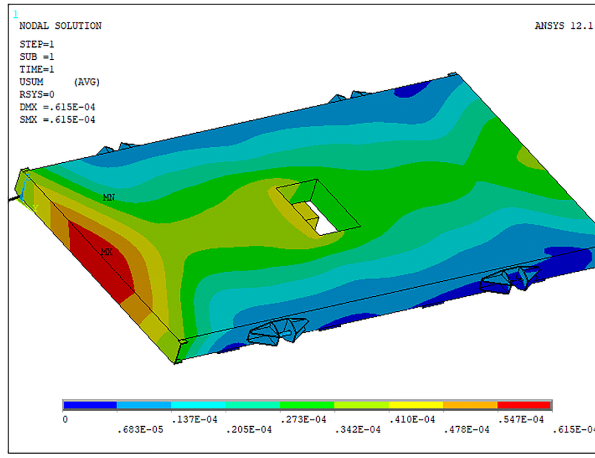

a

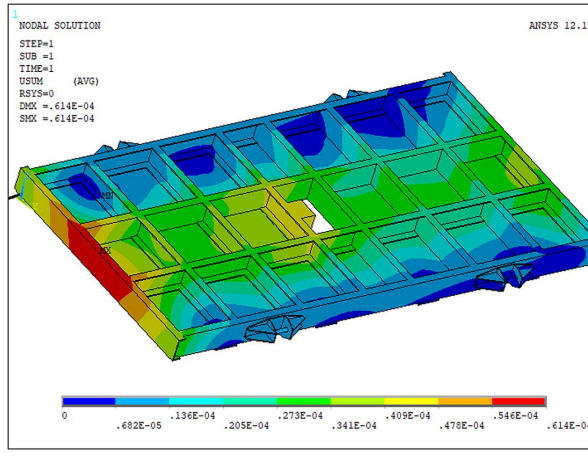

b

Fig. 8.28 Distribution of total displacements:
a – frames with a vertical vibrator; *b* – frames with
a vertical vibrator (the top sheet is conventionally not shown)

Movement in the vertical direction – along the *z*-axis, has both positive and negative values (**Fig. 8.29**), which indicates the presence of small deflections (0.0569 mm) on the cantilever sections of the frame and local bends on the side channels of the frame.

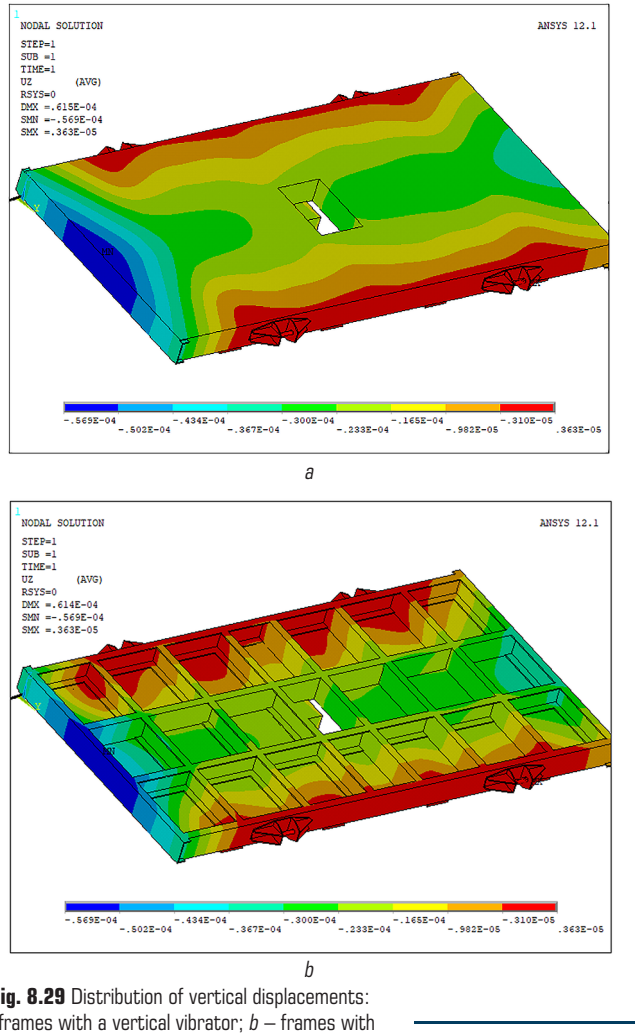

Fig. 8.29 Distribution of vertical displacements: *a* – frames with a vertical vibrator; *b* – frames with a vertical vibrator (the top sheet is conventionally not shown)

The highest values of the equivalent stress reach 10.6 MPa (**Fig. 8.30**). They are observed in the places where vertical and horizontal channels are welded at the place where the vibrator is attached. The values of these stresses are less than the maximum standard stresses, which indicates that the strength of the welded seams is ensured.

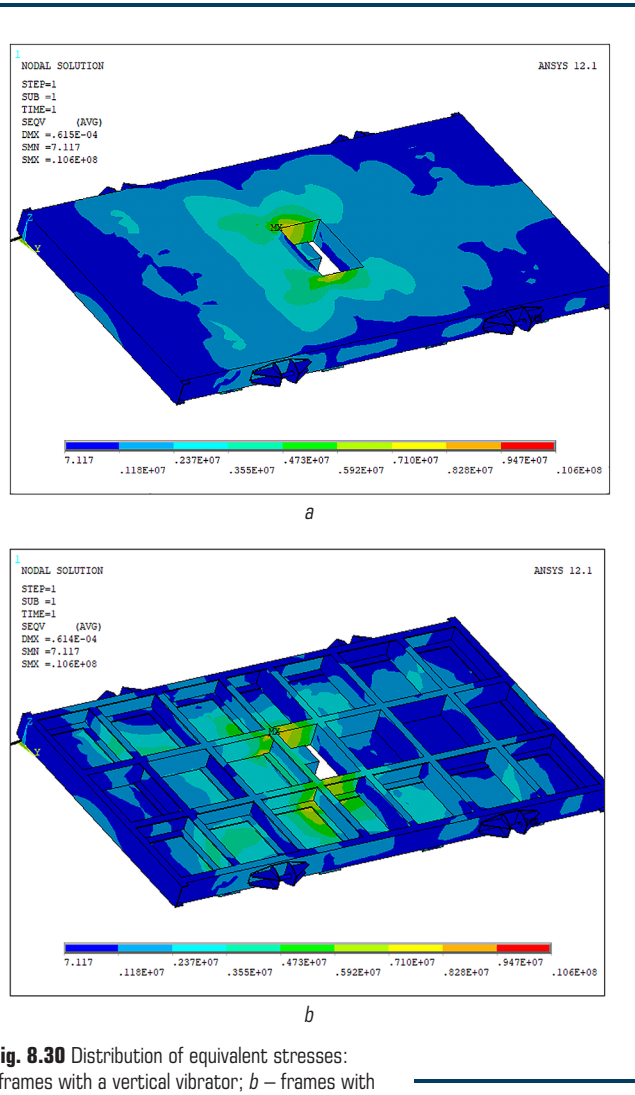

Fig. 8.30 Distribution of equivalent stresses: *a* – frames with a vertical vibrator; *b* – frames with a vertical vibrator (the top sheet is conventionally not shown)

In the direction of the *X* axis, the distribution of displacements is circular in nature, with a maximum (0.042 mm) at the place of load application; the outermost parts of the frame are the least deformable.

The distribution of stresses in the frame elements is uneven. The concentration of stresses is observed in the places of welding of elements, but the stress raisers have small values of 4.12 MPa in comparison with the ultimate strength of steel.

The stress in the direction of the *X* axis is distributed circularly, similar to the distribution of displacements. Moreover, the highest stress values are observed in the two nearest cells to the place of load application.

8.3.3 VIBRATION PLATFORM WITH HORIZONTAL VIBRATOR

The structure of the vibration platform VPGP-6.3×3.6 (**Fig. 8.32**) includes a movable frame with overall dimensions in plan 6.28×3.66, made of channels and a steel sheet made of calm-melting steel st.3sp. In the windows of the moving frame, vibration plates with welded-on M30 nuts are rigidly attached. On the moving frame there are rigid transverse stops for fixing the form with the concrete mixture. The vibration exciter is bolted to the movable frame. With the help of a V-belt transmission, the vibration exciter shaft rotates from an electric motor with a power of 30 kW. The windows of the movable frame are closed with metal covers that prevent particles of the concrete mixture from entering the platform's vibration drive. The movable frame rests on 8 rubber-metal supports attached directly to the foundation of the vibration platform. The supports are attached to the moving frame with the help of protrusions on the supports entering the mounting holes in the moving frame.

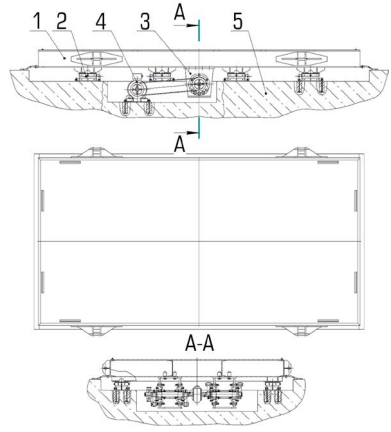

Fig. 8.31 Vibration platform VPGP-6.3×3.6 for the formation of ribbed slabs of coatings with the dimensions of the movable frame in the plan of 6.3×3.6 m: 1 – movable frame, 2 – elastic support, 3 – vibration exciter of torsional vibrations, 4 – electric motor, 5 – foundation

The vibration platform model was loaded with the same uniformly distributed load, but the design and direction of vibration movement were changed.

For this option, a deformed diagram, a displacement distribution diagram (**Fig. 8.32**) and a stress distribution diagram (**Fig. 8.33**) were also obtained.

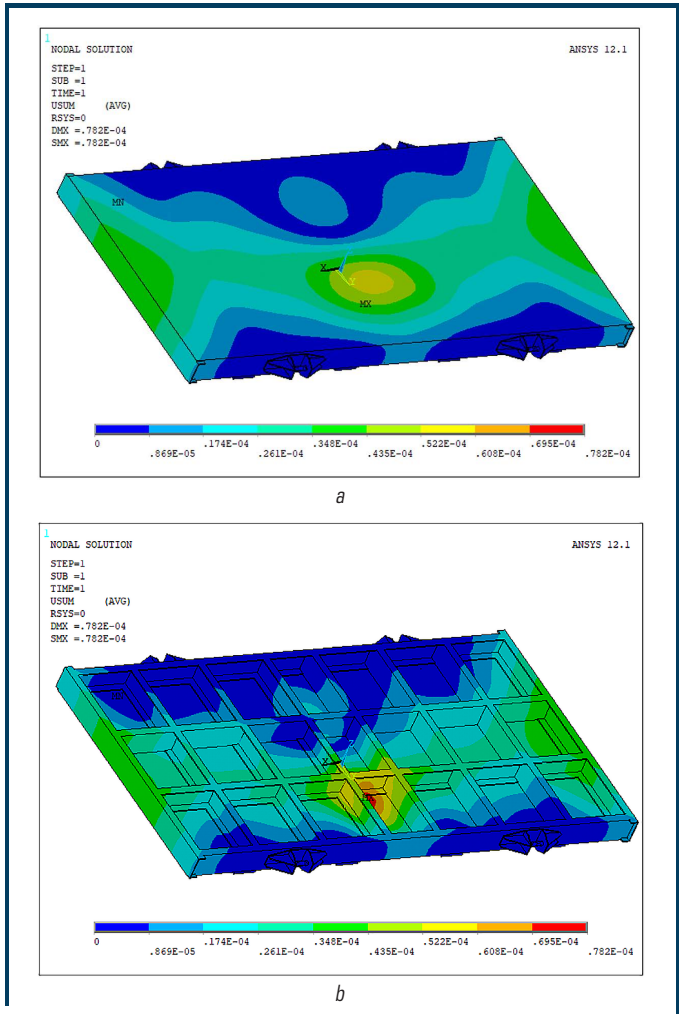

Fig. 8.32 Distribution of total displacements: *a* – frames with a horizontal vibrator; *b* – frames with a horizontal vibrator (the top sheet is conventionally not shown)

The most total displacements of the frame elements are 0.0782 mm (the area is marked in red in the diagram). Such deflections occur in the side channels of the frame on the cantilever sections free from supports (**Fig. 8.33**). In the center of symmetry of the frame, local deflections of up to 0.0608 mm are also observed.

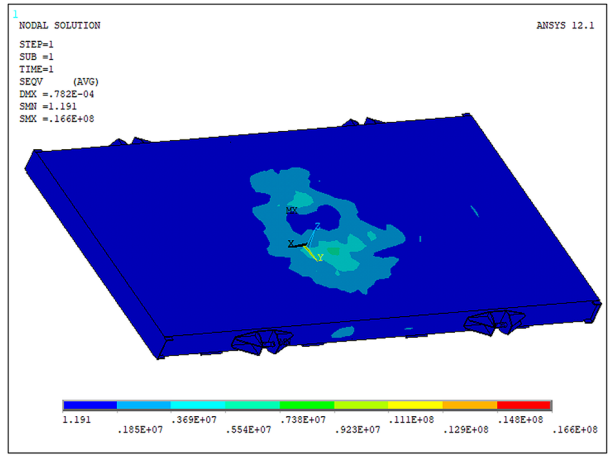

Fig. 8.33 Distribution of equivalent stresses: *a* – frames with a horizontal vibrator; *b* – frames with a horizontal vibrator (the top sheet is conventionally not shown)

Equivalent stresses have a maximum value of 16.6 MPa (**Fig. 8.33**). These values can be seen in the channels located above the frame supports and in the welds at the vibrator attachment points.

Dynamic calculation of the form [10] (**Fig. 8.34**) is performed in the ANSYS/LS-Dyna finite element analysis program. The program simulates the compaction of a mixture in a metal form during the operation of a shock-vibration unit. For the numerical model, two types of finite elements are used that implement the elastic and plastic properties of the metal form and mixture (**Fig. 8.35**).

The force resulting from the fall of the form from a height of 8 mm, taking into account the acceleration of gravity and the static and dynamic action of the loader on the metal form, is taken as the maximum load.

Fig. 8.34 Metal form

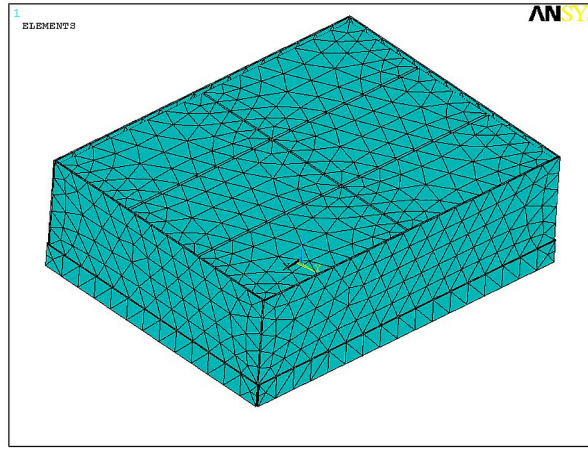

Fig. 8.35 Numerical model of the form with wood concrete mixture

Fig. 8.37 shows the picture of stress distribution on a deformed structure diagram. The loader is not shown in the **Fig. 8.37**, since the distribution of stresses and strains in it is not important for the task at hand. As can be seen from the **Fig. 8.37**, the stress in the elements of the form is on average 15–60 kPa, and the subsidence of the concrete mixture during compaction is about 38 mm, as shown in the work.

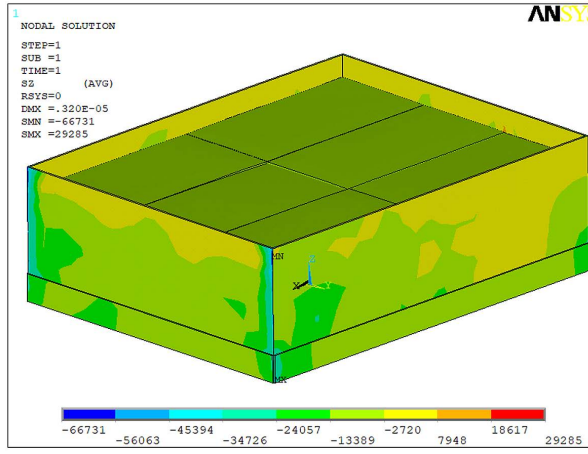

Fig. 8.36 Stress distribution in structural members

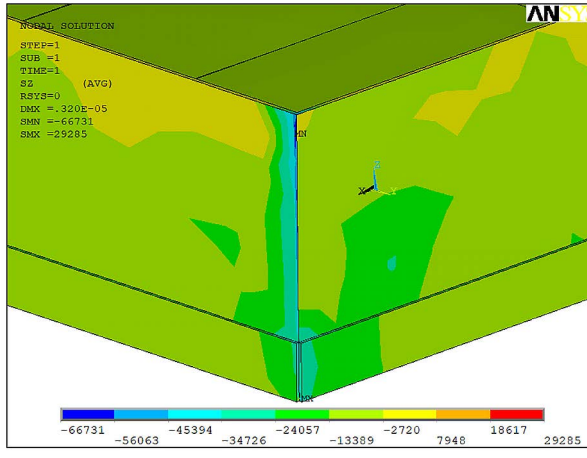

Fig. 8.37 Stress concentration at the corners of the form

The greatest deformation and stress concentration (60–65 kPa) occurs in the corners of the form, where the welded seams of the structure are located (**Fig. 8.37**).

8.4 INVESTIGATION OF THE STRESS-STRAIN STATE OF CRANES METAL STRUCTURES

The study of static dynamic loads of the slewing ring of a truck crane was carried out in order to establish the position of the system and its elements with the highest stresses. The basic laws of the theory of elasticity and plasticity were used to construct a computational mathematical model of a loaded support-rotary contour. Equations of motion were drawn up taking into account the behavior of structural elements and the machine as a whole under the simultaneous action of various loads. The design model was taken in the form of a structure consisting of rods rigidly connected to each other at the nodes. For each bar, this section is shown with geometric characteristics. As a calculation method, the finite element method was used with the definition of displacement (deformation), force (stress) at the mesh nodes of structural elements of the support-rotary contour. The distribution of stresses for each structural element was obtained depending on the type of load.

In the theoretical studies [7–11], a scientific hypothesis was proposed according to which the development of reliable and most efficient machines for various technological purposes is based on the establishment and general purposeful use of the regularities of changes in the internal properties of the working bodies of machines and the technological load, which is a processing material. The implementation of the hypothesis is provided by the solution of a scientific idea [11]. Recently, the development and creation of the design of machines for various technological purposes is carried out in the direction of searching for design solutions with a changing operating mode. In the process of operation of such machines, the maximum allowable use of the internal resources of the machine structure is assumed, which in turn necessitates ensuring strength and reliability with specified dynamic parameters. An integral assessment of the state of metal structures of the finished product can be carried out on the basis of dynamic tests. The idea of such tests is to find the actual dynamic characteristics of the structure (natural frequency, vibration amplitude, etc.) with the subsequent comparison of these characteristics with the characteristics obtained by the method of mathematical modeling of the given structure system. The mathematical model should be created in such a way as to adequately describe the real structure and its behavior under various loads, and also be able to reflect the modeling of various kinds of imperfections associated with manufacturing and direct operation as intended.

Under dynamic loads on structural elements inherent in most machines for technological purposes, the main type of damage is the formation and development of cracks due to the accumulation of fatigue stresses. Durability in case of tedious destruction is determined by the long-term cyclicity of the action of loads on the supporting structures of the machine and its individual elements, as a result of which a crack is formed, which gradually develops and leads to destruction.

The solution to the problem of determining the study of the stress-strain state is carried out by using an integrated approach that combines analytical calculations, mathematical modeling and experimental research directly.

For the implementation of these tasks, the following sequence of research was envisaged:

– analysis of the behavior of structural elements of the machine from the point of view of taking into account all types of loads that were carried out during its operation and determining the possible combination of loads acting on the elements;

– development of a computational model of the research object, taking into account the general or individual most loaded nodes or structural elements;

– drawing up equations of motion, taking into account the behavior of structural elements and the machine as a whole under the simultaneous action of various loads;

– assessment of real loads for the development of an algorithm for determining the stress-strain state, identification of the most stressed structural elements;

– development on a computer model of a matrix of control points for the limiting values of the integral characteristics of the state of the structure for subsequent use in field tests;

– carrying out computer calculations to determine stresses and strains by applying a number of possible loads to the model;

– development and implementation of experimental studies on samples reflecting the real operating conditions of a part or machine unit;

– adjusting the computer model until the comparison of the integral characteristics obtained by measurements at control points during the experiment and during simulation can differ from each other within the permissible error (the computer model obtained in this way will be adequate to the real design within the limits). points of adequacy – points of control of integral characteristics);

– development of recommendations for improving the existing or creating a new design, corresponding to the basic idea of the equal strength of stress distribution, regardless of the applied forces on the elements of the loaded product. The analysis of possible loads was carried out on the basis of the studies carried out using the example of truck cranes. This is due to the fact that these machines are a classic example of the structure of a system in which static and dynamic loads are organically combined, which require correct accounting for safe crane operation under real load conditions. The basic laws of the theory of elasticity and plasticity were used to construct a computational mathematical model of a loaded SC [11–14]. Equations of motion were drawn up taking into account the behavior of structural elements and the machine as a whole under the simultaneous action of various loads. In the case of a dynamic effect on its metal structure (**Fig. 8.38**) as a linear elastic body, the equations of motion in the adopted coordinate system (**Fig. 8.39**) are as follows:

$$z_{i,j,j} + F_i = \rho \cdot U_i, \tag{8.21}$$

where $z_{i,j,j}$ – stress tensors, (i, j=1, 2, 3); F_i – components of volumetric forces; ρ – material density; U_i – displacement vector.

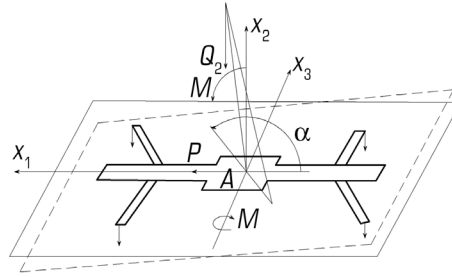

Fig. 8.38 Design diagram of the support contour of a truck crane

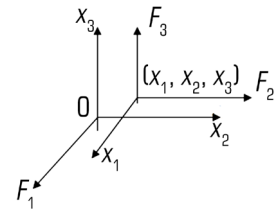

Fig. 8.39 Coordinate system of the acting forces on the support contour of the truck crane

If to take into account the viscous properties, then let's replace the operator from (21):

$$\rho \cdot \frac{\partial^2}{\partial t^2} \Leftrightarrow \rho \cdot \left(\frac{\partial^2}{\partial t^2} \right) + k \frac{\partial}{\partial t}, \tag{8.22}$$

where k – viscosity coefficient.

Equation (22) in this form remains unchanged.

Let's introduce designations for the speeds of wave propagation in the SC:

$$C_1^2 = \frac{1-v}{(1+v)(1-2v)} \cdot \frac{E}{\rho}; C_2^2 = \frac{1}{2(1+v)} \cdot \frac{E}{\rho}. \tag{8.23}$$

For the case when the force $F(t)$ is ordinary and acts along the $OX1$ axis (at the origin of the coordinate system):

$$U_1(x_1,x_2,x_3,t)=\frac{1}{4\pi\rho R}\times$$

$$\times\left[\frac{1}{C_1^2}\cdot\frac{x_1^2}{R^2}\cdot P\left(t-\frac{1}{C_1}\right)+\frac{1}{C_1^2}\cdot\left(1-\frac{x_1^2}{R^2}\right)P\left(t-\frac{1}{C_1}\right)-\left(1-3\frac{x_1^2}{R^2}\right)\cdot\int_{\frac{1}{C_1}}^{\frac{1}{C_2}}\lambda P(t-\lambda R)\mathrm{d}\lambda\right]; \quad (8.24)$$

$$U_2(x_1,x_2,x_3,t)=\frac{x_1x_2}{4\pi\rho R}\cdot\left[\frac{1}{C_1^2}\cdot P\left(t-\frac{R}{C_1}\right)-\frac{1}{C_1^2}\cdot P\left(t-\frac{R}{C_2}\right)+3\int_{\frac{1}{C_1}}^{\frac{1}{C_2}}\lambda P(t-\lambda R)\mathrm{d}\lambda\right]; \quad (8.25)$$

If the force acts along the *OX*2 axis, then it is necessary to replace the indices:

$$y(22)\Rightarrow\begin{cases}1\to 2;\\ 2\to 3;\\ 3\to 1.\end{cases}$$

If the force acts along the *OX*3 axis, then it is necessary to replace the indices:

$$y(22)\Rightarrow\begin{cases}1\to 3;\\ 2\to 1;\\ 3\to 2.\end{cases}$$

For a plane problem ($x3=0$); for a one-dimensional problem: ($x1\neq 0$; $x2=x3=0$).

The SC design scheme is taken in the form of a structure consisting of rods rigidly connected to each other at the nodes (**Fig. 8.40**) in a rectangular coordinate system *X*, *Y*, *Z* and is built along a line connecting the centers of gravity of the cross-sections of the rods.

Each element is designated by small circles numbered with Arabic numerals. The serial number of the bar (element) is shown in a circle. For each bar, this section is shown with geometric characteristics. As a calculation method, the finite element method was used with the definition of displacement (deformation), force (stress) at the nodes of the mesh of structural elements of the SC structure (**Fig. 8.41**).

The correctness of the results of mathematical modeling largely depends on the mechanical characteristics of structural materials and the study of the operation of complex assemblies of load-bearing structural elements. Experimental studies of the connection of parts to each other (**Fig. 8.42, *a***) and nodes (**Fig. 8.42, *b***) were carried out by the test method for determining the mechanical characteristics to check the results of analytical calculations. Tests on these stands allowed to propose the design of the elements used in real structures of the defense industry complex.

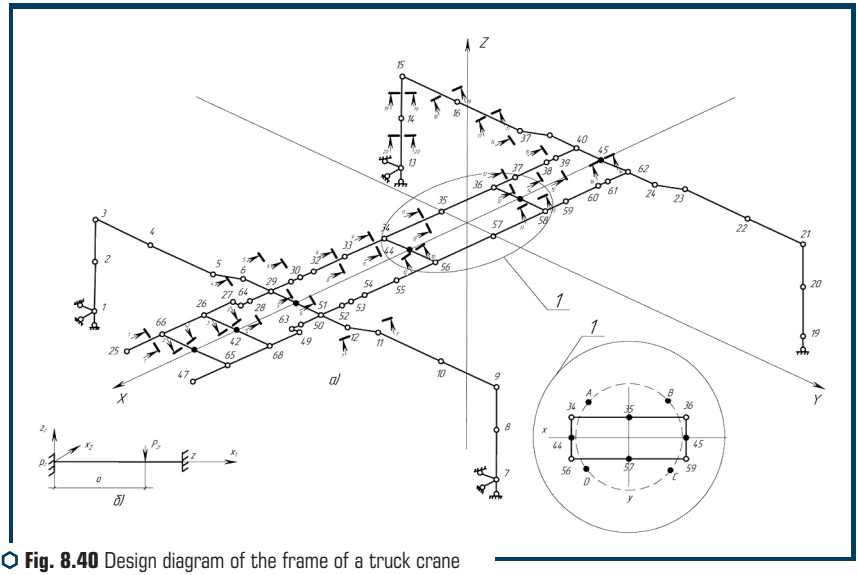

Fig. 8.40 Design diagram of the frame of a truck crane

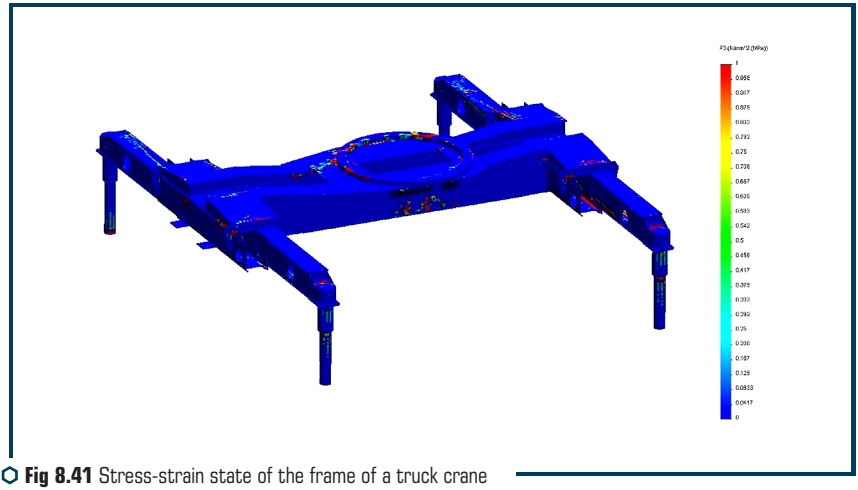

Fig 8.41 Stress-strain state of the frame of a truck crane

It is found that the maximum loads occur in the position of the crane unit perpendicular to the main axis of the vehicle on which the crane unit is fixed. At the same time, it is found that of all the nodes of the crane unit, the greatest stresses arise in the support contour (SC), which ensures the rotation of the lifting mechanism by 360 degrees.

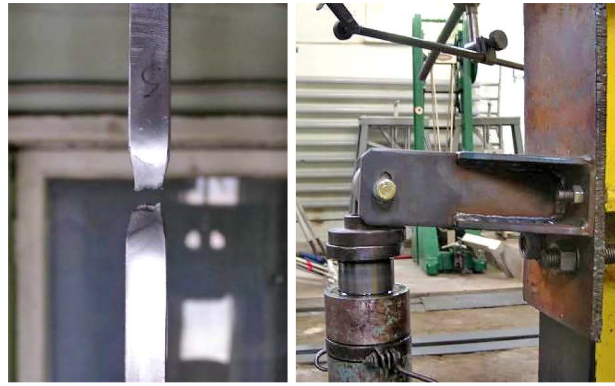

a *b*

Fig. 8.42 Testing of structural elements of metal structures: *a* – tensile welded joint; *b* – bracket test

By changing the dynamic and static loads and analyzing the results obtained, similar to **Fig. 8.41**, the research results were introduced into the SC structure in such a way that all the elements had the same order of numerical values of stresses, which in the final design solution made it possible to reduce the SC mass by 30 %.

8.5 DISCUSSION OF RESEARCH RESULTS

The research results (**Fig. 8.1**) indicate that the maximum values of the equivalent stresses of the forming surface are 2.5 MPa. Higher values of stresses are concentrated in the area of application and distribution of the driving force. The frame design accepts a maximum stress of 11.7 MPa (**Fig. 8.2**). The area of action of such stress values is limited by the contact zones of the frame with the supports and is of a local nature. Vibrograms of changes in the stresses of the forming surface are given for individual elements located near the application of a dynamic external force. This is a fundamentally new result. It consists in the fact that the detected transient process is intended to be taken into account when determining the parameters and locations of the vibrators. In such modes, the forms of natural vibrations of the system are realized with large vibration amplitudes and, accordingly, a lower frequency. And this opens up a real opportunity to reduce the energy consumption of the drives of the vibration machine. The stresses for structural elements located symmetrically on the opposite side from the applied force are investigated (**Fig. 8.5**). In contrast to the previous vibrograms, there is no in-phase change in stresses in relation to the forcing force, which confirms the inclusion of dissipative forces in the design model. An important

criterion for evaluating a design from the point of view of the efficiency of the compaction process is shear stress. Indeed, in the presence of such stresses in the medium, there is an intensive movement of particles and compaction. To analyze the shear stresses of the forming structure, time intervals were selected corresponding to 1/4 of the period of oscillation of the driving force (**Fig. 8.6**). The zones with the maximum positive stress values, in which the force is applied, have been determined. A complex sign-like stress-strain state of the structure under the action of a spatial load has been confirmed. This study has a limitation in terms of the adopted law of the change of dissipative forces.

A fundamentally new result has been obtained, which consists in the fact that the implementation of a complex vibration mode as an effective method of accelerated compaction of concrete mixtures is ensured by the arrangement of unbalances at a certain angle on each separate vibration unit. As a result, energy consumption is reduced by 30 %, and the process of forming a concrete product is reduced by 20 %. The presence of different forms of the polyphase spectrum is confirmed by the vibration modes (**Fig. 8.11–8.17**) and the distribution of the vibration amplitudes of the form surface along the length of the structure for one period of vibration. The use of such effects is determined by the overall dimensions of the product in terms of plan and height, which affects not only the phase deployment of the unbalances along the central axis of the vibration unit, but also the magnitude of the static moment of the unbalances.

The design diagram of an energy-saving vibration plant with a polyphase vibration spectrum has been substantiated. Modeling of the working process of a vibration plant is based on the use of the finite element method using the MSC.NASTRAN calculation complex (MSC.Software, Germany).

As a result of the research, the main modes of vibration have been determined by the numerical values of the frequencies of 1.32 Hz, 4.10 Hz, 16.61 Hz, 27.40 Hz. The calculated value of the oscillation frequency of the operating mode is 25 Hz. The most effective in the framework of the research carried out is the vibration form of 24.31 Hz. The implementation of this form of vibration provides an energy-saving mode of operation of the vibration unit.

A polyphase spectrum of vibrations of the unit has been established and proposedat an excitation frequency of 25 Hz, according to which vibration amplitudes of 0.27...0.6 mm are realized. The investigated vibration mode of the computational model is a confirmation of the energy-saving mode, which is a prerequisite for calculating and creating a new class of vibration unit.

Analysis of the stress-strain state of frames with horizontal and vertical vibrators shows that in the elements of the proposed frame structures during the operation of vibration platforms, stresses arise significantly less than the design resistance of steel, which provides the condition for the strength of the structure. The deflections in the frame elements are much less than permissible, which indicates the sufficient planar and spatial stiffness of the created frames and metal forms.

Frames with a vertically positioned vibrator work in tension and bending. The movements of the frame members are distributed circularly from the vibrator location. The greatest stresses arise at the welding points of the longitudinal and transverse channels and the top sheet in the vibrator attachment area. Their maximum values are 11.4 MPa.

For the distribution of displacements of frames with horizontally located vibrators, areas of both positive and negative deflections are characteristic. At the junction of the vibrator with the frame, a wave-like bend is observed, and in the cantilever sections, deflections of 0.0672 mm are observed. The maximum stress in the vertical direction is 16.6 MPa.

In the manufacture of frames of such structures, special attention should be paid to the quality of welded seams in the area of the vibrator and in the attachment points of the supports in order to minimize the possibility of cracks in them.

CONCLUSIONS TO SECTION 8

1. In the course of the research, finite element models of vibration machines have been developed to implement the transfer of energy in the vertical direction with a fixed frequency, with a polyphase direction of external forces, with a spatial direction of movement in the vertical and horizontal planes.

2. The study of the nature of the distribution and the numerical values of stresses and strains has been done in the forming structure of the unit, depending on the angle of instantaneous action of the external force of the vibrators and vibration frequencies.

3. The maximum values of the equivalent stresses of the forming surface are 2.5 MPa. Higher values of stresses are concentrated in the zone of application and distribution of force, the maximum stresses are 11.7 MPa.

4. The results obtained indicate the presence of vibration amplitudes of different shapes and numerical values over the area of a vibration unit with a polyphase vibration spectrum.

5. Stress concentrators in structural elements of machines for technological purposes have been determined, taking into account the working loads.

6. The static and dynamic loads of the support contour of a truck crane have been investigated.

7. The obtained research results are taken into account when making further design decisions when creating such machines.

REFERENCES

1. Petrov, A. A. (2002). Teoriia i proektirovanie vibratsionnykh mashin impulsnogo i rezonansnogo deistviia. Khmelnitskii: Tekhnologicheskii un-t Podoliia, 182.
2. Nazarenko, I., Gaidaichuk, V., Dedov, O., Diachenko, O. (2017). Investigation of vibration machine movement with a multimode oscillation spectrum. Eastern-European Journal of Enterprise Technologies, 6 (1 (90)), 28–36. doi: http://doi.org/10.15587/1729-4061.2017.118731
3. Bazhenov, V. A., Dashchenko, A. F., Orobei, V. F., Surianov, N. H. (2004). Chyselnie metodi v mekhanyke. Odessa: Draft, 564.

4. Bathe, K. J. (1996). Finite Element Procedures. New-York: Prentice Hall, 1037.
5. Lanets, O., Derevenko, I., Borovets, V., Kovtonyuk, M., Komada, P., Mussabekov, K., Yeraliyeva, B. (2019). Substantiation of consolidated inertial parameters of vibrating bunker feeder. Przeglad Elektrotechniczny, 95 (4), 47–52. doi: http://doi.org/10.15199/48.2019.04.09
6. Gursky, V., Kuzio, I., Lanets, O., Kisała, P., Tolegenova, A., Syzdykpayeva, A. (2019). Implementation of dual-frequency resonant vibratory machines with pulsed electromagnetic drive. Przegląd Elektrotechniczny, 95 (4), 43–48. doi: http://doi.org/10.15199/48.2019.04.08
7. Nazarenko, I. I., Nesterenko, T. M., Nesterenko, M. M., Marchenko, I. A. (2020). Kompiuterne modeliuvannia elementiv vibratsiinykh mashyn. Kompiuterna matematyka v nautsi, inzhenerii ta osviti (CMSEE-2020), 36–38.
8. Nazarenko, I. I., Smirnov, V. M., Fomin, A. V., Sviderskyi, A. T., Kosteniuk, O. O., Diedov, O. P., Zukhba, A. H.; Nazarenko, I. I. (Ed.) (2010). Osnovy teorii vzaiemodii robochykh orhaniv budivelnykh mashyn iz napruzheno-deformovanym seredovyshchem. Kyiv: «MP Lesia», 216.
9. Nesterenko, M. M., Nesterenko, T. M., Mahas, N. M. (2017). Method of calculation of shock-vibrating machinefor manufacturing products from light concrete for energy efficient reconstruction buildings in Ukraine. Naukovyi visnyk budivnytstva, 88 (2), 178–182.
10. Nazarenko, I. I., Dedov, O. P., Sviderski, A. T., Ruchinski, N. N. (2017). Research of energy-saving vibration machines with account of the stress-strain state of technological environment. The IX International Conference HEAVY MACHINERY HM 2017, 21–24.
11. Nazarenko, I., Gaidaichuk, V., Dedov, O., Diachenko, O. (2018). Determination of stresses and strains in the shaping structure under spatial load. Eastern-European Journal of Enterprise Technologies, 6 (7 (96)), 13–18. doi: http://doi.org/10.15587/1729-4061.2018.147195
12. Nazarenko, I., Gavryukov, O., Klyon, A., Ruchynsky, N. (2018). Determination of the optimal parameters of a tubular belt conveyor depending on such an economical. Eastern-European Journal of Enterprise Technologies, 3 (1 (93)), 34–42. doi: http://doi.org/10.15587/1729-4061.2018.131552
13. Luchko, J., Kovalchuk, V., Kravets, I., Gajda, O., Onyshchenko, A. (2020). Determining patterns in the stresseddeformed state of the railroad track subgrade reinforced with tubular drains. Eastern-European Journal of Enterprise Technologies, 5 (7 (107)), 6–13. doi: http://doi.org/10.15587/1729-4061.2020.213525
14. Kovalchuk, V., Onyshchenko, A., Fedorenko, O., Habrel, M., Parneta, B., Voznyak, O. et. al. (2021). A comprehensive procedure for estimating the stressed-strained state of a reinforced concrete bridge under the action of variable environmental temperatures. Eastern-European Journal of Enterprise Technologies, 2 (7 (110)), 23–30. doi: http://doi.org/10.15587/1729-4061.2021.228960